Wavefront sensing for WFIRST with a linear optical model

Alden S. Jurling*[ab] and David A. Content [a]
[a]NASA Goddard Space Flight Center 8800 Greenbelt Rd, Greenbelt MD 20771, USA
[b]Institute of Optics, University of Rochester, Rochester, NY 14627, USA

ABSTRACT

In this paper we develop methods to use a linear optical model to capture the field dependence of wavefront aberrations in a nonlinear optimization-based phase retrieval algorithm for image-based wavefront sensing. The linear optical model is generated from a ray trace model of the system and allows the system state to be described in terms of mechanical alignment parameters rather than wavefront coefficients. This approach allows joint optimization over images taken at different field points and does not require separate convergence of phase retrieval at individual field points. Because the algorithm exploits field diversity, multiple defocused images per field point are not required for robustness. Furthermore, because it is possible to simultaneously fit images of many stars over the field, it is not necessary to use a fixed defocus to achieve adequate signal-to-noise ratio despite having images with high dynamic range. This allows high performance wavefront sensing using in-focus science data. We applied this technique in a simulation model based on the Wide Field Infrared Survey Telescope (WFIRST) Intermediate Design Reference Mission (IDRM) imager using a linear optical model with 25 field points. We demonstrate sub-thousandth-wave wavefront sensing accuracy in the presence of noise and moderate undersampling for both monochromatic and polychromatic images using 25 high-SNR target stars. Using these high-quality wavefront sensing results, we are able to generate upsampled point-spread functions (PSFs) and use them to determine PSF ellipticity to high accuracy in order to reduce the systematic impact of aberrations on the accuracy of galactic ellipticity determination for weak-lensing science.

Keywords: WFIRST, phase retrieval, multi-field, weak-lensing, ellipticity, linear optical model, aberrations

1. INTRODUCTION

Previous work has shown that phase retrieval algorithms for image-based wavefront sensing [1,2,3,4] benefit greatly from using multiple defocused images as data rather than a single in-focus image. Even if an algorithm must work on a single image, a fixed defocus is preferable to purely in-focus images. This is partly because defocused images have much less dynamic range than in-focus images. This means that for a saturation-limited exposure, a defocused image can accept a longer exposure time (or a brighter source) without saturating and capture more total source photons. Thus, it achieves a higher average signal-to-noise ratio than an in-focus image. A second advantage is that the defocused image has more visible structure and shape over larger scales in the image. Finally, if focus diversity is employed rather than a fixed defocus, the robustness of the wavefront sensing algorithm significantly improves in terms of stagnation avoidance, stability and accuracy. A specific example of the benefits of focus diversity is the twin image problem: if the system's pupil is symmetric with respect to reflection through the origin, the phase solution from a single image will have a fundamental ambiguity: it may correspond either to a given solution or the same solution reflected through the origin and with the phase reversed in sign.

The advantages of focus diversity and defocused images for image-based wavefront sensing make it highly compelling, but requiring focus diversity also limits the systems where it can be applied and the operational scenarios where it can be useful. The requirement that most scientific applications of a telescope use in-focus images imposes the first fundamental limitation: If you require defocus for wavefront sensing, then wavefront sensing and science use of an instrument cannot occur at the same time. Since any time spent on engineering activities is a direct loss from science time (unless they can be scheduled while the telescope is otherwise unavailable, such as during a slew), the total time that can be allocated to wavefront sensing observations is limited. Even once engineering time is available for wavefront sensing, the limited time allocation imposes a trade between the number of defocused images and exposure time per image. If the wavefront sensing target stars are dim enough that they are not saturating in the available observing time (either due to well-depth or saturation avoidance in sample-up-the-ramp detection), this removes the inherent signal-to-noise ratio benefit for defocused images. In addition to the time required, there must be a mechanism to introduce the

Space Telescopes and Instrumentation 2012: Optical, Infrared, and Millimeter Wave, edited by Mark C. Clampin, Giovanni G. Fazio, Howard A. MacEwen, Jacobus M. Oschmann, Jr., Proc. of SPIE Vol. 8442, 844210
© 2012 SPIE · CCC code: 0277-786/12/$18 · doi: 10.1117/12.925089

Downloaded From: http://proceedings.spiedigitallibrary.org/ on 04/24/2014 Terms of Use: http://spiedl.org/terms

defocus (such as a detector motion or weak lenses in a filter wheel). If wavefront sensing is required frequently, that mechanism must be very robust. Finally even if the engineering time and mechanisms are available, defocusing for wavefront sensing is incompatible with science that requires continuous observation of the same target over an extended period.

Because of the costs of defocused and focus-diverse wavefront sensing, we are interested in developing an algorithm that can work on collections of in-focus images and still achieve the levels of accuracy and robustness we obtain from focus-diverse algorithms. In particular we are interested in wavefront sensing for the imager channel of WFIRST as specified in the IDRM report [5,6]. One of the major science applications of the WFIRST imager is a weak gravitational lensing survey, which requires making shape (ellipticity) measurements of millions of galaxies over a large area of the sky. Because the weak-lensing measurement requires very high accuracy, it is very sensitive to systematic errors introduced by aberrations in the imaging system changing the shape of PSF. Because it is impractical to design or build an imaging system that is corrected to within the required tolerances over a large field of view, it is instead necessary to know the system's field-dependent point-spread function so that it can be removed from the science data by deconvolution. If the system aberrations were static over time, it would be sufficient to measure the system aberrations once during the commissioning process and use that as a calibration over the life of the mission. In practice, the system's PSF will vary over time due to thermoelastic effects, as the telescope's thermal environment changes at different pointing angles, and additionally vary over much longer time scales as structures outgas and change shape slightly. Again because the scientific performance requirements for the weak-lensing measurement are so tight, these small dynamic errors are a concern; it is likely to require an ongoing monitoring process, with either continuous monitoring or periodic monitoring. Determining the time scale of variation and the required cadence of wavefront monitoring will require further thermal and mechanical monitoring which is not yet available, so for this paper we will assume pessimistically that wavefront sensing is required either continuously or with such a frequency that requiring dedicated defocused imagery for wavefront sensing would impose an unacceptably onerous overhead on science. Thus we conclude that using the primary science detectors for defocused wavefront sensing is not a suitable solution.

An alternate approach would be to use a separate instrument or channel for defocused wavefront sensing. The IDRM has only a single imager and two spectrometers (not suitable for high precision wavefront sensing), so this would require adding a separate instrument channel for wavefront sensing, with a commensurate increase in cost and complexity. Even if an auxiliary instrument suitable for wavefront sensing were in place, it would face several difficulties. The first is non-common path aberrations; if it does not share the same tertiary mirror as the imager or adds additional down-stream optics, its aberrations will not be the same as the imager's and any time dependent motion or deformation in the non-common elements of either channel will lead to errors in wavefront sensing, which are likely to exceed the acceptable limits for weak lensing. Second, an instrument with a narrow field of view will not be able to capture the full field-dependent aberrations that effect the imager; this is acceptable if the time-dependent aberrations are primarily uniform over the field of view, with the field-dependent aberrations relatively stable. Because of these issues we will not consider wavefront sensing by separate instruments. This leaves either dedicated engineering detectors in the imager (with either fixed or variable defocus) that can be used independently of the science detectors or using in-focus science data for wavefront sensing. Both are potentially reasonable approaches; in this paper we consider the second because it requires the least additional hardware.

Without access to focus diversity, we are left with two questions. First, how to recover the benefits of (phase) diversity in algorithmic robustness? Second, how to achieve high signal-to-noise ratios necessary to reach the required accuracy requirements imposed by weak-lensing science? In the case of WFIRST the answer to both of these questions is the same: exploit WFIRST's wide field of view. First, because the imager's field of view is much larger than its isoplanatic patch size, the field dependence of aberrations over the field of view introduces a form of phase diversity: two stars from different parts of the field of view will exhibit different aberrations from one another. If we can provide a model for this dependence, we can exploit it as a diversity mechanism in our algorithms. Second, again because the field of view is large, there are many bright unresolved stars in the field of view. If we can jointly fit all or many of these stars rather than a handful of defocused images from a single star, we can achieve very large gains in overall signal-to-noise ratio, allowing us to achieve high accuracy in the wavefront fits.

In order to realize the benefits of field diversity, we need a parameterized model of the field dependence of the system aberrations; if each star were allowed to have a fully independent wavefront realization, there would be no gain in robustness or signal-to-noise ratio. Since we are considering a particular system and have access to the optical design, a prescription retrieval [7] model seems appropriate. That is, we parameterize the field dependence in terms of the

Downloaded From: http://proceedings.spiedigitallibrary.org/ on 04/24/2014 Terms of Use: http://spiedl.org/terms

mechanical degrees of freedom (both rigid body and figure error) of the optical surfaces in the system, and we search for a mechanical configuration that is consistent with the observed images. Because the number of mechanical degrees of freedom is far smaller than the number of stars times a reasonable number of low-order wavefront terms, this represents a large reduction in search space compared to the independent image problem.

Having selected the mechanical degrees of freedom as our search space, we must still determine how to model their relation to the field dependence. Design and performance assessment for optical systems are typically done with real ray trace models of the system. However, non-linear optimization-based phase retrieval algorithms benefit greatly from the use of analytic gradient techniques, and it is not obvious how to incorporate a ray trace model into this process without imposing a potentially unacceptable computational cost. Because the merit functions in phase diversity are much more expensive to compute than a lens design error function, a direct finite difference gradient computation that might achieve acceptable performance for the design problem is much more difficult for wavefront sensing. The ideal solution from a wavefront-sensing standpoint would be an analytic representation of the field-dependent aberrations of the system, produced through an extension of aberration theory to non-rotationally-symmetric and misaligned systems, such as [8] or [9, 10]. Such an analysis including both rigid body and figure terms is not available for WFIRST at the time of this writing, so we have adopted a linear optical model (LOM) [11] to represent the field dependence.

The LOM is essentially a first-order sensitivity analysis of the optical design; the design is ray traced in an optical design code, and then small perturbations are made to the parameters and retraced; this allows the linear dependence of phase in the exit pupil of the system to be calculated by finite differences. Note that this is linear in mechanical perturbation, not in the functional form of the field dependence of the aberration, which can include higher order dependences on the field angle, provided they occur in this small-perturbation limit. Given these sensitivities and the exit pupil aberration maps for the configuration space point where the LOM was generated, a field-dependent wavefront error map can be generated for a given mechanical realization of the system. For our simulations the LOM was generated at the perfectly aligned case, but in practice *a priori* known static misalignments could be included, giving a LOM that was accurate in the region of configuration space near the known point. In order to speed computation in the wavefront sensing process, we further projected the first order wavefront sensitivities onto a low order Zernike wavefront basis. For a given field point, the linear optical model can be stored as a N x M matrix L_n, where N is the number of mechanical degrees of freedom (78 in our case) and M is the number of Zernike terms used for the low-order expansion. Thus the forward model, converting mechanical configuration points x to a Zernike coefficient map for the nth field point is a simple matrix multiplication followed by an addition of the known constant bias (the design residual aberrations, in our case):

$$y_n = L_n x + b_n \tag{1}$$

If we assume the total joint phase retrieval error metric is given by

$$E = \sum_n w_n E_n \tag{2}$$

then, given the analytic gradients of E with respect to the vector components of y_n, via the chain rule [12] for partial derivatives [7A] we can compute the gradient with respect to x by a matrix multiply with the transpose of the linear optical model matrix and a sum over the field points;

$$\nabla_x E = \sum_n w_n L_n^T \left(\nabla_{y_n} E_n \right). \tag{2}$$

Because the LOM matrix is relatively small compared to the array sizes used to model the optical fields, the addition of these two steps in the forward and gradient model for the wavefront sensing algorithm adds negligibly to the total computational cost of the algorithm, which is dominated by computing the Fourier transforms needed to propagate complex fields between the pupil and image planes.

The linear optical model formalism provides us a simple and computationally efficient method for multi-field wavefront sensing and prescription retrieval. Because it is based on a first-order analysis at a given point in the design space, it is not applicable for systems that are expected to see large changes in mechanical state, which would involve higher order dependencies on the mechanical configuration not captured in the LOM. However, because the design of the WFIRST imager calls for a system that is both well corrected and very stable, we expect that once the telescope has been aligned

Downloaded From: http://proceedings.spiedigitallibrary.org/ on 04/24/2014 Terms of Use: http://spiedl.org/terms

and commissioned on orbit, using the LOM to model small deviations from the static on-orbit alignment should be reasonable.

2. MODEL MATCHING REQUIREMENTS

Two major factors limit the quality of wavefront retrievals for phase retrieval algorithms: model matching and noise. Model matching refers to how well the physical optics simulations in the forward model agree with the actual physical world. This depends both on computational and software resources and on knowledge of the system. For example, when modeling the physical aperture stop of the system in the computer, it is necessary to discretize the continuous aperture, which introduces a mismatch between the model and the real world. This error can be reduced by using shaded edges and/or more finely sampling the pupil. Similar issues apply in selecting the sampling in the image domain and in discretizing the continuous wavelength band for a broadband system into finite wavelengths. Even given noise-free data, these approximations will limit the ultimate accuracy of the algorithm and introduce a trade between desired accuracy and computational burden. Because of the combination of high accuracy requirements and the extremely multi-field nature of the WFIRST imager, the computational requirements for an adequately model matched phase retrieval model for WFIRST will be substantial. For that reason, rather than undertake a comprehensive exploration of the model matching requirements, we have considered a single aspect of the model matching problem, discussed below.

We assessed the impact and sensitivity to model matching by exploring one particular dimension of this problem, the sensitivity to the particular choice of wavelengths in a broadband phase retrieval model. Figure 1 shows results of a simulation to address this. The vertical axis shows the error in the ellipticity computed from the retrieved point spread functions, while the horizontal axis shows the true (total) ellipticity of the point spread functions. Each marker represents a single realization of the phase retrieval problem: particular aberrations and noise. We considered monochromatic data matched to a monochromatic model, as well as polychromatic models with 10 and 13 discrete wavelengths. For the polychromatic wavelengths, we considered both matched and mismatched cases (in the matched cases the same wavelengths are used in the data simulation and retrieval; in the mismatched, we simulated with 13 and retrieved with 10 or simulated with 10 and retrieved with 13). On average the matched cases (Monochromatic data with monochromatic retrieval, polychromatic 10 wavelength data with polychromatic 10 wavelength data, and polychromatic 13 wavelength data with polychromatic 13 wavelength model) perform similarly well, while all of the mismatched (polychromatic 10 wavelength data with polychromatic 13 wavelength model and 13 wavelength polychromatic data with 10 wavelength polychromatic model) cases perform comparatively poorly.

The direct conclusion from this is that 10 discrete wavelengths is not a sufficient to model the point spread functions accurately enough that the errors in the phase retrieval results introduced by discretizing the spectra are smaller than the noise-limited accuracy at our signal levels: if N wavelengths is sufficient to model the point spread functions with required accuracy, than data simulated with more than N wavelengths should be adequately retrieved by a model with only N wavelength, which we do not see here. The more general conclusion from this is that is likely that other computational aspects of the problem will require high accuracy and that the overall computational difficulty of the problem will be significant.

3. NOISE LIMITED PERFORMANCE

In the remainder of the paper, we will focus on noise-limited performance. That is, we will ask the question: assuming the modeling match issues are all dealt with, at a given noise level, what is the achievable wavefront sensing performance? Simulations addressing this topic may use lower fidelity models than would be required to adequately fit real-world data by simply making the same approximations in the phase retrieval forward model that are used in the simulation of the 'measured' data. As an example of this, we adopt throughout a 64x64 grid across the clear aperture of the system to reduce computational cost, recognizing that in practice much finer sampling will be required.

Although for computational reasons we must use simplified models as discussed above, it is important to establish that the overall trends we observe in our simulations are consistent with the trends in higher fidelity models. In order to investigate this, we have considered simulations using both monochromatic and polychromatic data. We show that in both cases, when the phase retrieval model is matched to the data simulation model, the final reconstruction accuracy is the same in either case. We also limited the number of field points we considered, both to reduce the computational cost of modeling many field points and because only a finite grid of points are computed in our LOM.

Downloaded From: http://proceedings.spiedigitallibrary.org/ on 04/24/2014 Terms of Use: http://spiedl.org/terms

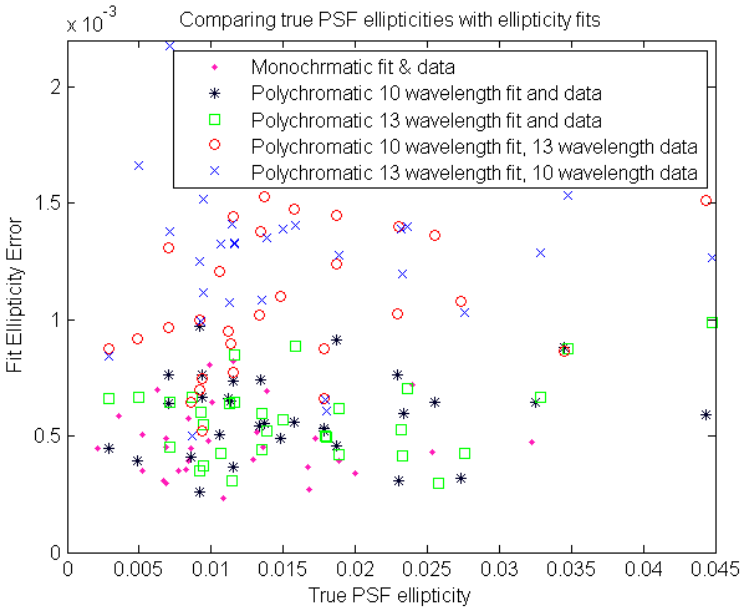

Figure 1. Retrieval accuracy for monochromatic and polychromatic simulations with different numbers of images. [todo: revise figures for print]

However, we would like to able to extrapolate from this scenario to one with a more realistic number of stars. Based on photon noise statistics, we expect the residual wavefront error to go as one over the square root of the number of photons (for equally bright stars this is proportional to the total number of stars). In order to test this assumption, we simulated cases where we used dithering at the existing points to simulate the noise impact of having more than 25 single stars. That is, for one field point in our LOM, we generated several (10 in this case, for a total of 250 PSFs) point spread functions with different sub-pixel displacements and noise realizations as a proxy for having more than the 25 field points computed in our LOM. In all these cases, we observe that the final phase-retrieval accuracy depends on the total photon budget in the image plane, not these particular modeling choices, as shown in Figures 2 and 3; this gives us confidence that the photon noise limits established in this approximate regime will have relevance to more realistic systems. In particular, the performance is consistent with the expected one over square root dependence on the total number of photons; in Figure 3 we fit that model to the observed performance points. Figure 4 shows representative simulated data for a single field point along with the corresponding phase-retrieval fit, as well as a noise-free version of the PSF and upsampled versions of both the true and fit point-spread functions. We can see that despite the aliasing and noise in the data for individual field points, in the joint retrieval we have been able to reconstruct the underlying diffraction-limited point-spread function with high accuracy.

4. PHOTON BUDGET CONSIDERATIONS

The model fit in Figure 3 lets us extrapolate from the cases considered so far to scenarios with larger numbers of stars as we would expect in a full flight scenario. This is based on the assumption that all modeling matching requirements are met and that photon noise statistics continue to dominate phase retrieval accuracy, so that an accuracy estimate based only on the total photon budget is a reasonable estimate. Our model fit for ellipticity accuracy is 1.5 / sqrt(total photons). Using a simple star frequency spread sheet for the vicinity of the galactic pole, we can estimate a total of 3×10^8 photons from stars between 12th and 20th magnitudes in a 120 sec exposure over a 1.6 μm to 2.0 μm band, for an estimated ellipticity error of 8.7×10^{-5} if all available stellar sources are used for wavefront sensing. The IDRM weak-lensing program requires knowledge of PSF ellipticity to $4.7 \times 10e^{-4}$, so it is at least plausible that an algorithm of the type described in this paper working on a single frame of science data would be able to achieve the required accuracy. This should not be taken as a precise prediction of real performance in practice, but rather as a plausibility argument that the

Downloaded From: http://proceedings.spiedigitallibrary.org/ on 04/24/2014 Terms of Use: http://spiedl.org/terms

approach we have outlined in this paper is basically suitable to the problem at hand and that further development of this approach and more detailed simulation studies are warranted to establish more realistic error bounds.

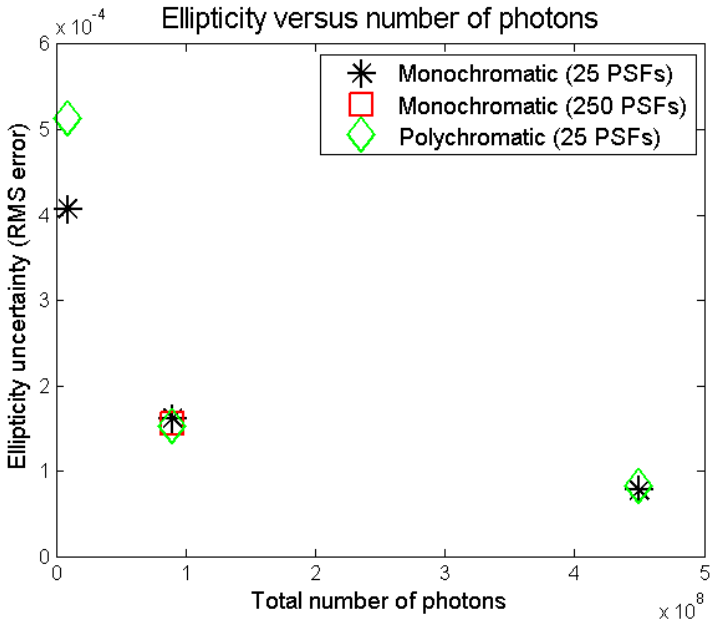

Figure 2. Retrieval accuracy for monochromatic and polychromatic simulations with different numbers of dithered images in terms of total number of photons. The ellipticity uncertainty shown on the vertical axis is the average over a Monte Carlo simulation.

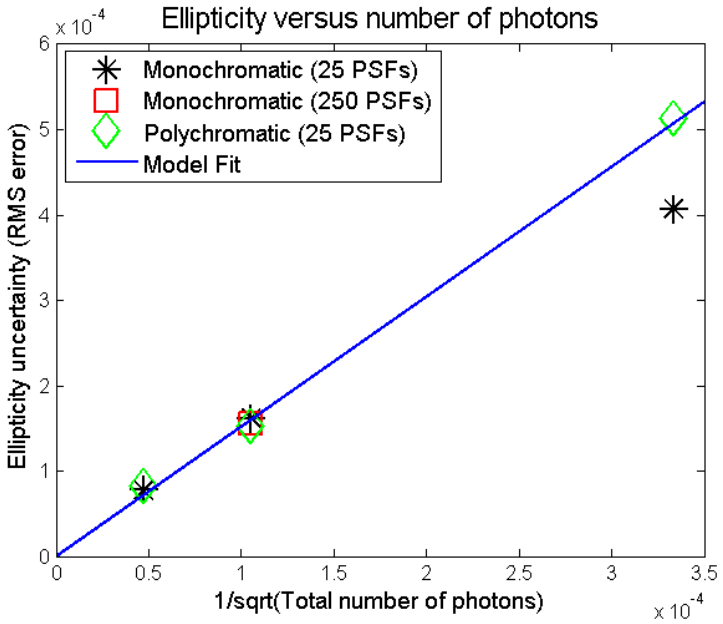

Figure 3. Retrieval accuracy for monochromatic and polychromatic simulations with different numbers of dithered images, fit to inverse square root model we expect based on photon noise. In this figure we have rescaled the horizontal axis so that the square root of total number of photons dependence appears a linear.

Downloaded From: http://proceedings.spiedigitallibrary.org/ on 04/24/2014 Terms of Use: http://spiedl.org/terms

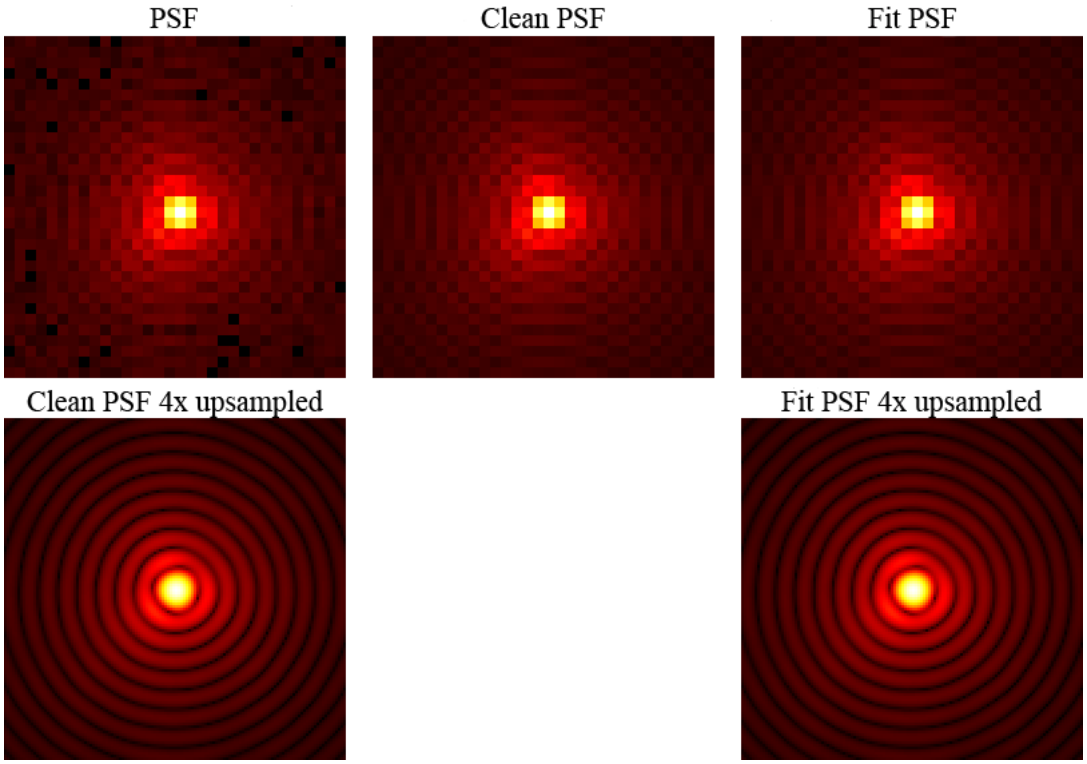

Figure 4. Real and recovered point spread functions. Note that the PSF structure is much more apparent in the upsampled fit PSF than the original data, showing the advantage of a wavefront sensing fit over trying to deconvolve with measured PSFs directly. All PSFs are shown at intensity to the 0.25 power.

5. CONCLUSIONS

We have developed a multi-field phase retrieval algorithm optimized to the requirements of the WFIRST IDRM imager instrument and weak-lensing science program. Our algorithm uses in-focus images of stars over a wide field of view. The field-dependent aberrations of the system act as a form of phase diversity and substitute for focus diversity in this context. Because of the extremely large field of view for WFIRST, there will be many stars available for wavefront sensing in a given exposure and there will be significant change in the wavefront aberrations over the full field of view. We show that even with undersampled (for intensity) images and no focus diversity, we can achieve phase retrieval accuracy competitive with state of the art focus-diverse phase retrieval results. This is due to large number of simultaneously imaged stars available when using the full field of view of a wide-field telescope like WFIRST. We have also shown that, based on a simple photon budget calculation, it is plausible that our algorithm can achieve the required weak-lensing accuracy working from a single data frame.

6. ACKNOWLEDGEMENTS

Thanks to Prof. James R. Fienup and Jennifer M. Jurling for assistance in preparation and proofing of this manuscript. Thanks to the WFIRST project team for providing mission background information. Thanks to Joe Howard for the WFIRST LOM. Thanks to Paul Schechter and Chris Hirata for insight into the WFIRST weak lensing program. Thanks to the members of the GFSC Wavefront Sensing and Control group and the members, past and present, the of Fienup research group at the University of Rochester, for many helpful discussions.

Downloaded From: http://proceedings.spiedigitallibrary.org/ on 04/24/2014 Terms of Use: http://spiedl.org/terms

REFERENCES

[1] Fienup, J. R., Marron, J.C., Schulz, T. J., and Seldin, J. H., "Hubble Space Telescope characterized by using phase retrieval algorithms," Appl. Opt. **32**, 1747-1767 (1993).

[2] Fienup, J. R. "Phase-retrieval algorithms for a complicated optical system," Appl. Opt. **32**, 1737-1746 (1993).

[3] Fienup, J. R. "Phase retrieval algorithms: a comparison," Appl. Opt. **21**, 2758-2769 (1982).

[4] Brady G.R., and Fienup, J.R. "Nonlinear optimization algorithm for retrieving the full complex pupil function," Opt. Express **14**, 474-486 (2006)

[5] Green, J., Schechter, P., et al, "Wide-Field InfraRed Survey Telescope (WFIRST) interim report", 11 July 2011, http://wfirst.gsfc.nasa.gov/science/WFIRST_Interim_Report.pdf

[6] Content, D. A., Mentzell, J. E., Goullioud, R. and Lehan, J. P., "Optical design trade study for the Wide Field Infrared Survey Telescope [WFIRST]", Proc. SPIE 8146, 81460Y (2011)

[7] Redding, D.C. et al, "Optical state estimation using wavefront data", Proc. SPIE **5523**, 212 (2004).

[8] Schechter, P. L., and Levinson, R. S., "Generic misalignment aberration patterns in wide-field telescopes," Publications of the Astronomical Society of the Pacific, Volume **123**, issue 905, pp.812-832

[9] Thompson, K. "Description of the third-order optical aberrations of near-circular pupil optical systems without symmetry," J. Opt. Soc. Am. A **22**, 1389-1401 (2005).

[10] Thompson, K., Schmid, T. and Rolland, J., "The misalignment induced aberrations of TMA telescopes," Opt. Express **16**, 20345-20353 (2008).

[11] Howard, J. M., Kong, Q. H., Shiri, R., Smith, J. S., Mosier, G. and Muheim, D., "Optical modeling activities for NASA's James Webb Space Telescope (JWST): Part V. Operational alignment updates", Proc. SPIE **7017**, 70170X (2008)

[12] Riley, K. F., Hobson, M. P., Bence, S. J., [Mathematical Methods for Physics and Engineering], Cambridge University Press, Cambridge U.K. & New York U.S.A.

Downloaded From: http://proceedings.spiedigitallibrary.org/ on 04/24/2014 Terms of Use: http://spiedl.org/terms